Energy 49 (2013) 434–443

Contents lists available at SciVerse ScienceDirect

Energy

journal homepage: www.elsevier.com/locate/energy

Geometric arrangement and operation mode adjustment in low-enthalpy geothermal borehole fields for heating

Markus Beck [a,*], Peter Bayer [b], Michael de Paly [a], Jozsef Hecht-Méndez [c], Andreas Zell [a]

[a] University of Tübingen, Wilhelm-Schickard-Institute for Computer Science (WSI), Sand 1, 72076 Tübingen, Germany
[b] ETH Zürich, Engineering Geology, Sonneggstrasse 5, 8092 Zurich, Switzerland
[c] University of Tübingen, Center for Applied Geoscience (ZAG), Sigwartstraße 10, 72076 Tübingen, Germany

ARTICLE INFO

Article history:
Received 11 June 2012
Received in revised form
24 October 2012
Accepted 28 October 2012
Available online 9 December 2012

Keywords:
Shallow geothermal energy
Multiple BHEs
BHE positioning
Optimization
Evolutionary algorithms
Linear programming

ABSTRACT

The efficient operation of ground source heat pump (GSHP) systems with multiple borehole heat exchangers (BHEs) over a lifetime of decades implies an optimized performance of the BHEs and a mitigation of the environmental impact of the system. This paper introduces a new combined optimization approach, which adjusts the BHE positions as well as the individually regulated energy extraction for each single BHE within a given borehole field in conduction dominated media for a given seasonal changing load profile. The optimization of only the BHE positions without optimizing the individual BHE loads nearly produces the same improvement of the underground temperature change of approximately 12% as an optimization of the BHE loads without optimized positioning. The combination of both optimization approaches results in only slightly better results compared to a result achieved by only one of the optimization approaches. Thus for homogeneous fields without groundwater flow, an optimal load assignment can be substituted by an optimal BHE placement, which leads to a considerably reduced complexity of the borehole field.

1. Introduction

Direct geothermal energy use is a popular way of managing the space heating and cooling demand of buildings [1–3]. In most applications, energy is extracted or injected at near-ground level (<400 m) by borehole heat exchangers (BHEs) [4–8]. These commonly represent vertical boreholes, in which a working fluid flows up- and downward in a pipe. The pipe is connected to an aboveground heat pump, and both together are called ground coupled or ground source heat pump (GSHP) systems [9–11]. The majority of GSHPs are applied for heating. The heat pump extracts energy from the fluid to raise the temperature of the space heating system. It concentrates the extracted heat and thus enables warm water production by decreasing the carrier fluid only by a few degrees [12,13]. This Carnot process is most energy-efficient if the temperature step from inlet to outlet of the heat pump is held low. Therefore, significant ground cooling by permanent or seasonal energy extraction should be avoided [11,14–16]. Borehole heat extraction is achieved by creation of a radial temperature gradient towards the BHE, thus acting as an energy sink. The intensity of conductive heat flow to the BHE is governed by the properties of the ambient ground, and when described in steady-state by Fourier's law it is limited by the effective thermal conductivity [17]. Excessive heat transfer by a steeper gradient is undesirable to avoid ground freezing, to minimize ecological impacts and to keep the heat pump efficiency at a high level [18–21].

When planning BHEs, the task is essentially to determine which volume of the subsurface needs to be penetrated to provide the energy that is extracted over a period of usually decades efficiently and sustainably. Higher volumes are accessed by combined use of several longer, more costly BHEs, which are often limited in depth by depth-dependent drilling costs, geological or regulative constraints. Hence, substantial thermal energy requirements, such as for large residential houses, geothermal district heating systems, office buildings, schools or industrial applications are provided by fields of multiple adjacent BHEs [13,22–27]. While the planning of GSHPs with single BHEs follows standard practices, design and operation of multiple BHEs is still not routine. This is because neighboring BHEs potentially interact, and ground energy supply to BHEs at the center of the field may be reduced by those BHEs that act as shields on the outer field positions.

In standard applications, multiple BHEs are operated parallel, with equal flow velocity of the circulating heat carrier fluid. As heat extraction is controlled by the in-situ temperature gradient

* Corresponding author. Tel.: +49 7071 2978979; fax: + 49 7071 295091.
E-mail address: m.beck@uni-tuebingen.de (M. Beck).

0360-5442/$ – see front matter © 2012 Elsevier Ltd. All rights reserved.
http://dx.doi.org/10.1016/j.energy.2012.10.060

towards each BHE, cooler regions that evolve in the center of a field produce less heat. This means local cooling at individual BHEs automatically mitigates heat extraction and thus this automatism regulates a balanced energy extraction from the ground. Still, the open question remains: is equal flow operation for given geometric arrangements optimal, and does improvement potential exist by systematic control of the BHE-specific heat carrier flow velocities, which ultimately yield BHE-specific energy extraction loads? In Ref. [28], we suggested operating multiple BHEs with different energy extraction loads so as to increase the outer BHE loads on the expense of those in the center. The loads in a hypothetical borehole field, with 25 BHEs arranged in a fixed grid as illustrated in Fig. 1, were adjusted time-dependently for long-term seasonal energy extraction. As an objective, we selected the minimization of the maximal temperature decrease in the ground. Accordingly, solutions are searched for with balanced extraction of heat, without local cooling of the ground, and thus with technical as well as environmental improvements in comparison to standard practice. The field was simulated by superimposed line-source equations and automatically optimized using linear programming. It was demonstrated that depending on the seasonal heating energy requirements, complex symmetric optimal loading patterns evolve with temporally variable operation of the BHEs over the entire operation period of 30 years. It was also shown that the maximum decline of the temperature in the field could be mitigated by 18%. The advantage of linear programming for tuning BHEs in a given geometric (usually grid) arrangement was also demonstrated in Ref. [29] for conditions with substantial groundwater flow.

In Refs. [28,29], computationally efficient analytical models, which simulate the thermal conditions in the ground for given BHE loads, are used for the simulation-optimization step. In order to compare to standard practice, the optimized scenarios are examined in ex-post analyses by numerical models and compared to equal flow operation. A main finding was, that even if the flows are not implicitly subject to optimization, using the loads as surrogate leads to improved BHE operation modes. As an alternative, candidate solutions could be evaluated by numerical simulation, but the associated computational burden is immense [30,31] and depending on the runtime of the numerical model, satisfactory optimization may be impossible.

In the present study, we build up on our previous work and suggest a second optimization step, which, additional to load optimization, adjusts BHE positions within the field. For the optimization of the BHE positions we select a variant of Evolutionary Algorithms, Differential Evolution (DE). In preliminary analyses on BHE positioning with numerical [30] and analytical models [32], DE revealed to be a suitable algorithm for solving the associated complex positioning problem. Both optimization steps are applied individually, sequentially, or combined to conclude upon the most favorable overall optimization strategy. As a simulation approach, the temporal and spatially superimposed finite line-source equation is chosen, which is considered more accurate than the infinite variant [28], in particular for depth-limited BHE installation. The analytically optimized fields are then compared in a numerical ex-post analysis using the Superposition Borehole Model (SBM). SBM was first introduced by Eskilson [33] for simulating closed systems with one or multiple boreholes and was upgraded by Pahud et al. [34]. It is based on finite differences and capable of calculating the three-dimensional temperature field in the ground for such a system. Boreholes are organized in symmetry groups, which allow an aggregation of multiple boreholes in parallel or serial connection. Different loads and heat carrier fluid flow velocities can be applied individually to the BHEs, and hence this program is ideally suited for detailed examination of different borehole fields. SBM has been validated in several applications in practice [35] and is an established numerical model in theoretical studies (e.g. Ref. [28]).

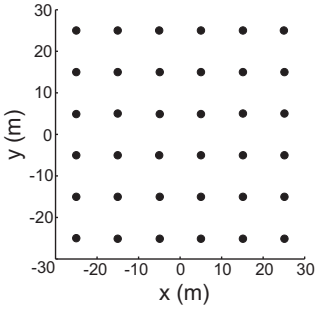

Fig. 1. Grid arrangement of BHEs in an area of 50 m × 50 m.

In the following, first the governing equations to describe the heat transfer processes when operating multiple BHEs are presented, and then the simulation procedures are explained. They are employed to a field of 36 BHEs, which is oriented at common conditions in practice. It serves as a case study for testing the different optimization strategies. We will distinguish six different strategies and, as a reference, the grid-shaped (Fig. 1) arrangement with equal flow operation. They are compared with respect to robustness and the quality of the found solutions. Finally, the borehole field solutions are inspected for characteristic features in order to generalize the findings for the planning of other borehole fields.

2. Methods

2.1. Simulation of multiple BHEs

An efficient method for calculating the radial temperature change ($\Delta T = T_u - T$) in the subsurface caused by a single vertical BHE is the finite line-source model [33,36]:

$$\Delta T(\Delta x, \Delta y, \Delta z, t, q) = \frac{q}{4\pi\lambda}\left[\int_0^L \frac{1}{r}\operatorname{erfc}\frac{r}{\sqrt{4\alpha t}}dz' - \int_{-L}^{0}\frac{1}{r}\operatorname{erfc}\frac{r}{\sqrt{4\alpha t}}dz'\right] \quad (1)$$

where T_u is the undisturbed temperature of the underground at time t, and L is the borehole length. T is the altered temperature, q is the given energy transfer rate per unit length of the BHE, or load. $\Delta x = (i - x_k)$ and $\Delta y = (i - y_k)$ are the distances to an arbitrary location (i,j) with respect to a BHE located on the z-axis at (x_k,y_k,z') with $\Delta z = (z - z')$ and $r = \sqrt{\Delta x^2 + \Delta y^2 + \Delta z^2}$. Two case specific ground thermal properties are included, namely α, which is the thermal diffusivity, and λ, which is the bulk thermal conductivity. Parameters α and λ are assumed to be constant and describe a finite homogeneous and isotropic medium.

A premise for the applicability of the line-source equation is that the ground thermal properties do not depend on temperature [5], resulting in a linear relationship of q and ΔT. Due to the fact that energy is an extensive and additive variable [37–41], the superposition principle can be applied to Eq. (1) as:

$$\Delta T_{i,j}\left(t, q_{k=1,\ldots,n}\right) = \sum_{k=1}^{n}\Delta T_k(i - x_k, j - y_k, \Delta z, t, q_k) \quad (2)$$

where n is the number of BHEs and T_k is the temperature change at (i,j) in a depth z caused by BHE k with an energy transfer rate q_k

located at (x_k,y_k). When the workload q varies over time, it can be considered as a series of heat pulses (temporal superposition). This superposition already been demonstrated in related studies [29,33,40–43]. The variable energy extraction is subdivided into m time steps with constant load:

$$\Delta T\left(\Delta x,\Delta y,\Delta z,t,q_{l=1,\ldots,m}\right)=\sum_{l=1}^{m}\frac{q_l-q_{l-1}}{4\pi\lambda}\left[\int_0^L\frac{1}{r}\mathrm{erfc}\frac{r}{\sqrt{4\alpha(t_m-t_l)}}\mathrm{d}z'-\int_{-L}^{0}\frac{1}{r}\mathrm{erfc}\frac{r}{\sqrt{4\alpha(t_m-t_l)}}\mathrm{d}z'\right] \tag{3}$$

where m is the total number of time steps and q_l is the load during time step l which runs from t_{l-1} to t_l, with $q_0=0$ and $t_0=0$.

The combination of Eqs. (2) and (3) allows for an estimation of the temperature change at any arbitrary location in the subsurface exerted by multiple BHEs, each with different time variable energy loads:

$$\Delta T_{i,j}\left(t,q_{k\ldots n,l\ldots m}\right)=\sum_{l=1}^{m}\sum_{k=1}^{n}q_{k,l}\omega_{k,l}^{t,i,j}(i-x_k,j-y_k) \tag{4}$$

with

$$\omega_{k,l}^{t,i,j}(\Delta x,\Delta y)=\frac{1}{4\pi\lambda}\left(\left[\int_0^L\frac{1}{r}\mathrm{erfc}\frac{r}{\sqrt{4\alpha(t-t_{l-1})}}\mathrm{d}z'-\int_{-L}^{0}\frac{1}{r}\mathrm{erfc}\frac{r}{\sqrt{4\alpha(t-t_{l-1})}}\mathrm{d}z'\right]-\left[\int_0^L\frac{1}{r}\mathrm{erfc}\frac{r}{\sqrt{4\alpha(t-t_l)}}\mathrm{d}z'-\int_{-L}^{0}\frac{1}{r}\mathrm{erfc}\frac{r}{\sqrt{4\alpha(t-t_l)}}\mathrm{d}z'\right]\right) \tag{5}$$

as the response factor of BHE k on a position (i,j) within the BHE field at time step $l\in 1,\ldots,m$ with reference to the current time step $t\in 1,\ldots,m$; given that $l\le t$, $\Delta x=(i-x_k)$, $\Delta y=(j-y_k)$ and $\Delta z=(z-z')$.

For a better manageability we merged the BHE loads and the response factors into vectors $\vec{q}=(q_{1,1},\ldots,q_{n,1},\ldots,q_{n,m})$ and $(\omega_{1,1}^{t,i,j},\ldots,\omega_{n,1}^{t,i,j},\ldots,\omega_{n,m}^{t,i,j})$. In this way, Eq. (4) is expressed as

$$\Delta\vec{T}_{i,j}(t,\vec{q})=\vec{q}\left(\vec{\omega}^{t,i,j}\right)^T \tag{6}$$

$\Delta\vec{T}_{i,j}(t,\vec{q})$ is the temperature change in the underground on position (i,j) at time step t caused by the superposition of all BHEs in the field with the temporal load pattern $\vec{q}$.

2.2. Setup of study case

The optimization procedure is tested on a case study, which is grounded in reality, where 36 BHEs of 100 m depth each are installed within a 50 m × 50 m area. In grid arrangement (Fig. 1), the grid distance between adjacent BHEs is 10 m. This follows a standard value in practice and is slightly higher than the recommended 7–8 m distance for such a field [44]. The geological setting, as described in Table 1, is assumed to be water-saturated and the ground is approximated as homogeneous, isotropic media. Groundwater flow is negligible and thus heat in the ground is only transported by conduction. The entire borehole field is operated for 30 years in seasonal heating mode, with a specific energy extraction of BHEs according to the German Engineer Association (VDI) guideline for thermal use of the ground [45]. A monthly variable heating demand is supplied, which reaches 216 MWh in one year (Fig. 2). The seasonal heat demand is derived based on a specific heat transfer rate of 33 W m^{-1} and an annual runtime of 1800 h [45]. It is assumed to resemble conditions typical for a GSHP system in Central Europe.

2.3. Objective function and constraints

Heat extraction is least efficient in cooled ground regions. Therefore, in accordance with Refs. [28,29], an objective function is formulated to avoid substantial local cooling of the ground:

$$\text{minimize}\left(\max\left(\Delta\vec{T}_{i,j}\right)\right) \tag{7}$$

The optimized solution is a borehole field that keeps the induced peak cooling of operating BHEs, max($\Delta T_{i,j}$), as small as possible. Thus, a balanced heat extraction from the ground is achieved. For one constellation of BHEs, P, the objective function for the optimization procedure is defined as:

$$F_{\mathrm{opt}}(P)=\mathrm{argmin}\left[\max\left(\Delta T_{i,j}(t)\right)\right]\quad\forall\,(i,j,t)\in S \tag{8}$$

where S is a set of all spatial and temporal measurement points, defined by 3-tuples (i,j,t). Furthermore, an equality constraint is introduced:

$$E_l=\sum_{k=1}^{n}q_{k,l}\quad l=1\ldots m \tag{9}$$

This warrants that the total extracted energy from all BHEs, i.e. the sum of the loads, $q_{k,l}$, equals the claimed energy per time step l. The superimposed finite line-source equation, Eq. (6), is applied for simulation of ground temperature changes in the borehole field. Most significant changes are noticed in the individual BHEs that act as heat sinks. The line-source assumes an infinitely small cross section of a BHE, which is unrealistic and thus not applicable to simulate the exact thermal conditions within a borehole. Instead, we suggest examining the temperature only at a specified small radius around each BHE, which is then used to evaluate the objective function. Experience shows that inspecting the temperature at a few discrete points around each BHE is sufficiently accurate to approximate the ambient thermal regime. Four reference points at a radius of 0.5 m are chosen here, when the analytical equation is applied (Fig. 3).

Table 1
Parameter specifications for the simulation-optimization procedure.

Parameter	Value (analytical model)	Value (numerical model, SBM)
Operation period	30 y	30 y
Ground porosity	0.46	–
Ground volumetric heat capacity	2.4 × 10^6 J m^{-3} K^{-1}	
Ground thermal conductivity (λ)	1.70 W m^{-1} K^{-1}	
Ground thermal diffusivity (α)	8.83 × 10^{-7} m^2 s^{-1}	–
Length of borehole (L)	100 m	
Total volumetric pumping rate of heat carrier fluid in BHE	–	0.018 m^3 s^{-1}

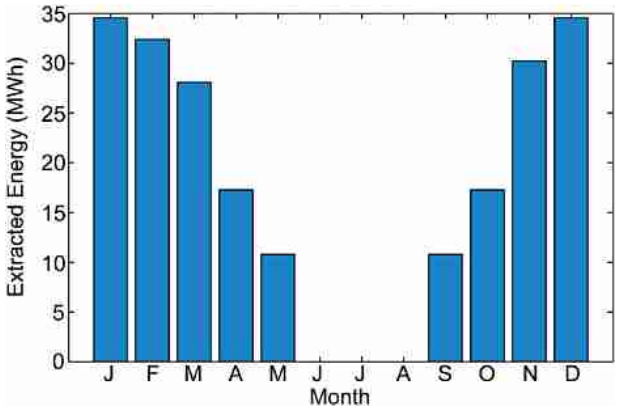

Fig. 2. Annual variation of generated heating energy for the simulated GSHP system of the study case with 1800 operating hours per year. The number of simulated BHEs is 36, with an average specific energy extraction of 33 W m^{-1} per BHE.

Averaging $\Delta T_{i_{1,\ldots,4} j_{1,\ldots,4}}$ at the four points $(i_{1,\ldots,4} j_{1,\ldots,4})$ allows estimating a mean subsurface temperature $\Delta T_{i,j}$ at the borehole wall for each BHE at each time step l. This is achieved fast with the analytical model used for optimization. However, when inspecting the optimized solutions in more detail with a numerical model after the optimization procedure, reference points have to be coordinated with the numerical grid. This means, in these ex-post simulations with the numerical simulation routine SBM, circular arrangement of temperature reference points around BHEs is hardly possible. SBM facilitates inspecting an arbitrary number of field cuts for desired time segments during the simulation time. One cut defines a rectangular area at user-defined depth parallel to the surface of the earth, which in x- and y-direction is divided into a user-defined number of segments. Since reference points are only available on a pre-defined mesh, consistent proximal temperatures are only possible for BHEs arranged on a grid with same mesh size as that of the reference points. In this special case, distances between nodal reference points and BHEs are the same. However, this is not valid when BHE positions are adjusted by automatic optimization. Unequal distances will potentially bias the estimation of the thermal regime in the vicinity of BHEs.

To diminish this effect, we define a 0.2 m high resolution mesh for the reference points. Instead of 4 points, as done for analytical simulation, for each BHE at position (x_k,y_k) we define eight reference points $i_{k,1,\ldots,8} j_{k,1,\ldots,8}$, which are evenly distributed on a circle with a radius of 0.5 m around the BHE position (Fig. 4). The temperature differences $\Delta T_{i_{k,1,\ldots,8} j_{k,1,\ldots,8}}$ are approximated by linear interpolation between the temperature values of the neighboring mesh nodal points.

The effective load along the BHE depends on the temperature of the surrounding ground and consequently varies with the depth.

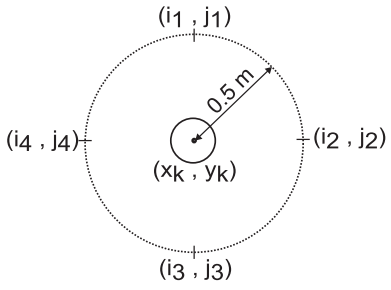

Fig. 3. Location of the four reference points around each BHE used for calculating a representative average borehole wall temperature.

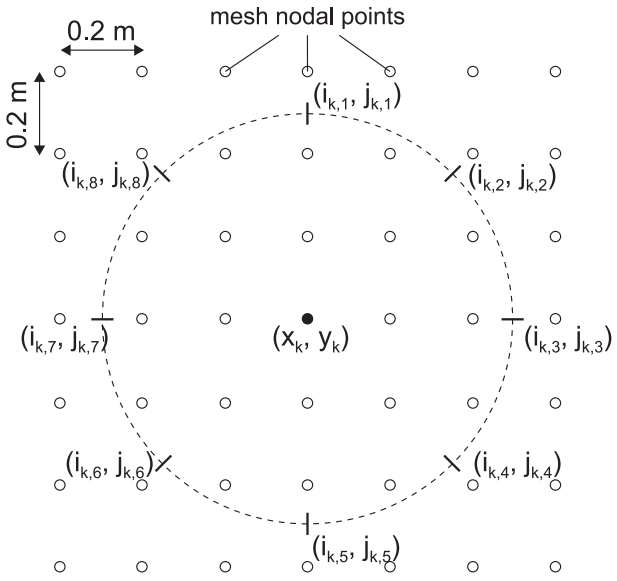

Fig. 4. Location of the eight reference points around each BHE used for estimating the subsurface temperature during the ex-post numerical simulation step.

Thus, the highest heat flow between ground and BHE will be at the axial ends of the pipe, while the least heat flow will be in the central zone. Eq. (1) shows that the finite analytical model assumes the same load q and the same heat flow for every examined depth z, while the numerical model SBM calculates the fluid flow in the pipe and a variable load depending on the depth. The consequence is that the analytical model overestimates the ground cooling around the central pipe, while temperature changes at the axial ends of the pipe will be underestimated. More detailed numerical simulation, for instance by Florides et al. [46] reveals that in the case of heat extraction, strongest cooling occurs close to the inlet and to the side of the input tube. The main question thus, is if the chosen fast but approximate analytical simulation procedure is sufficiently accurate to guide the optimization and what error is introduced by treating the BHE as a line-source. In a preliminary analysis with the studied BHE fields we found, the discrepancies between the computed temperatures by analytical and numerical models are $<$0.2 K, which is considered acceptable for an operation period of 30 years. For the selected scenarios, ground temperature values calculated by SBM for different depths (25 m–95 m) in 0.5 m distance to the borehole vary only in a range of $<$1.0 K. This error is even reduced when choosing $z = 15$ m for the analytical model to approximate the "true" 50 m temperatures, as predicted by the numerical model.

2.4. Optimization of BHE positions

Eqs. (5) and (6) indicate that the temperature $\overrightarrow{T}_{i,j}$ at a position (i,j) is a non-linear function of the BHE position (x_k,y_k). Concerted adjustment of BHE positions thus requires a non-linear optimization technique that ideally can deal with non-convexities of the objective function. The BHE positioning problem can be compared to finding optimal well layouts for groundwater extraction, which has been intensively studied previously [47,48]. The associated objective functions are typically complex and have numerous local optima. Evolutionary algorithms, meanwhile, are the most commonly used global search procedures for solving such problems. Based on previous results [30,32], Differential Evolution (DE) is chosen for the present study. In detail, the variant DE/current-to-best/1 with the algorithm specific tuning parameters $F = 0.8$

(differential weight), $C_r = 0.6$ (cutoff probability) and a population size $n = 30$ is applied. This DE variant turned out to achieve the best average performance and highest robustness. DE is a stochastic search procedure. Accordingly, to draw statistically significant conclusions, repeated applications to the same problem are required. Here, we employed the DE 20 times with 50,000 objective function calls for each run.

2.5. Optimization of the energy extraction rates of BHEs

By the load optimization step, seasonally variable loads are assigned individually to the BHEs in the field. This is applicable independent of their geometric arrangement, and consequently, loads can be optimized for a grid, an arbitrary or pre-optimized BHE layout. Since the temperature $\overrightarrow{T}_{i,j}$ at position (i,j) linearly depends on the loads, $\overrightarrow{q}$, linear programming is selected for optimization. In comparison to the more demanding stochastic optimization of positions, this step is computationally efficient and also ensures finding the global optimum. We introduced this linear programming procedure in our previous study [28]. Depending on the field thermal parameters, the inertia of the system and the given load pattern, in some cases the maximum overall ground temperature change may not be influenced by the load assignment for certain time steps, and thus will not be captured by the first objective. Thus, to include these cases, a second objective, which additionally minimizes the maximum temperature change within every single time step l, is introduced:

$$\text{minimize}\left(\sum_{l=1}^{m}\max\left(\Delta\overrightarrow{T}_{i,j}(l,\overrightarrow{q})\right)\right) \tag{10}$$

To obtain a single objective function, Eqs. (7) and (10) are combined to:

$$\text{argmin}\left(w\cdot\max\left(\Delta\overrightarrow{T}_{i,j}(t,\overrightarrow{q})\right)+\sum_{l=1}^{m}\max\left(\Delta\overrightarrow{T}_{i,j}(l,\overrightarrow{q})\right)\right) \tag{11}$$

$\forall\,(i,j,t)\in S$. The weighting factor w ensures a high priority of the primary objective over the second objectives and is set to 100 in this study. The problem of assigning optimal BHE loads, which minimize the temperature change in the ground, can be formulated as a linear program. It is, amongst others, constrained by the energy demand for each time step, which can be expressed as the equality constraint defined in Eq. (9). A more detailed explanation of the structure of the linear program can be found in Refs. [28,32].

2.6. Combined optimization/simulation procedure and problem simplification

Optimized solutions will be symmetric due to isotropic heat transport. This can be anticipated for load and position optimization, given that the field area is symmetric, like the rectangle of the study case. When loads are adjusted for fixed grid arrangement, the 36 BHEs can be subdivided in four mirror symmetric quadrants of 9 BHEs each.

Four quadrants can also be distinguished when positions are optimized. As shown in the example in Fig. 5, each BHE has three corresponding BHEs in the other three quadrants of the field. All corresponding BHEs have the same load q_t for each given time step t, and the BHEs coordinates can be mapped onto each other by mirroring along the symmetry axis of the field. Thus, in a rectangular field centered at (0,0), four BHEs 1…4 exist with:

$$q_1 = q_2 = q_3 = q_4 \tag{12}$$

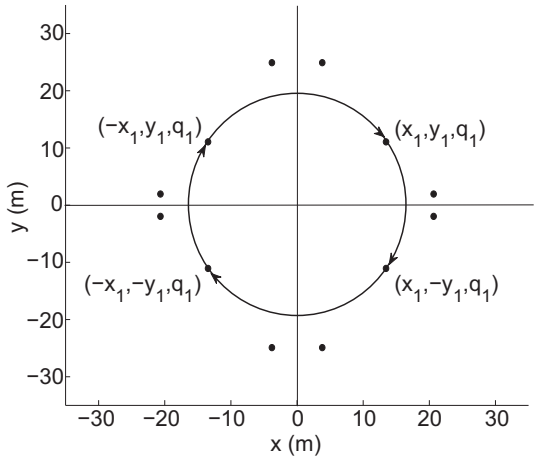

Fig. 5. Exploitation of the symmetry of rectangular borehole fields for dimensionality reduction.

$$(x_1,y_1) = (x_2,-y_2) = (-x_3,y_3) = (-x_4,-y_4) \tag{13}$$

This relationship allows for the reduction of the dimensionality of the optimization problem to one fourth, which is a straightforward step to speedup the optimization process.

A main goal of this study is to compare different optimization strategies, and by this, develop a recipe for efficient borehole field planning and operation. The two main choices are optimization of loads and of positions. They can be exclusively applied, sequentially or combined. Additionally, we want to compare performance of borehole fields with optimized loads to those operated at equal flows, as is standard in practice, when the heat carrier fluid velocity is not regulated. This leads us to six different strategies (Fig. 6), which subsequently will be compared:

(1) The “grid equal flow” option involves no optimization. BHEs are arranged on a uniform grid and equal flows are applied. The flows are adjusted for each month to supply the energy demand as given in Fig. 2. This variant serves as reference and simulates the standard.
(2) The “grid load optimization” alternative represents the variant which was introduced in Ref. [28]. For a given (uniform grid) arrangement, loads are optimized by linear programming.
(3) The “sequential optimization” strategy starts with optimization of the BHE positions by the Evolutionary Algorithm (DE). During this step, all BHEs are charged the same loads. The optimized field geometry is selected for the second optimization step, where the loads are optimized. Main interest is in the additional improvement potential of a borehole field that has already been geometrically adjusted.
(4) For comparison with the sequential optimization strategy (3), a variant “position optimization with equal flow” that only involves the first step, that is, position optimization, is defined. Instead of optimized loads, the BHEs are operated with equal flow in the numerical ex-post simulation. This variant will also reveal the difference between exclusively load-optimized (2) and exclusively position-optimized solutions.
(5) The “combined optimization” strategy follows the most demanding route, and can be expected to exploit the maximal optimization potential. Here, for each BHE geometry tested with the DE, the loads are adjusted by linear programming. This means only load-optimized candidate solutions are taken for objective function evaluation with the DE.
(6) In this “equal flow” variant, the solutions of (5) are run with equal flows. This case serves as control case for strategy (5) to

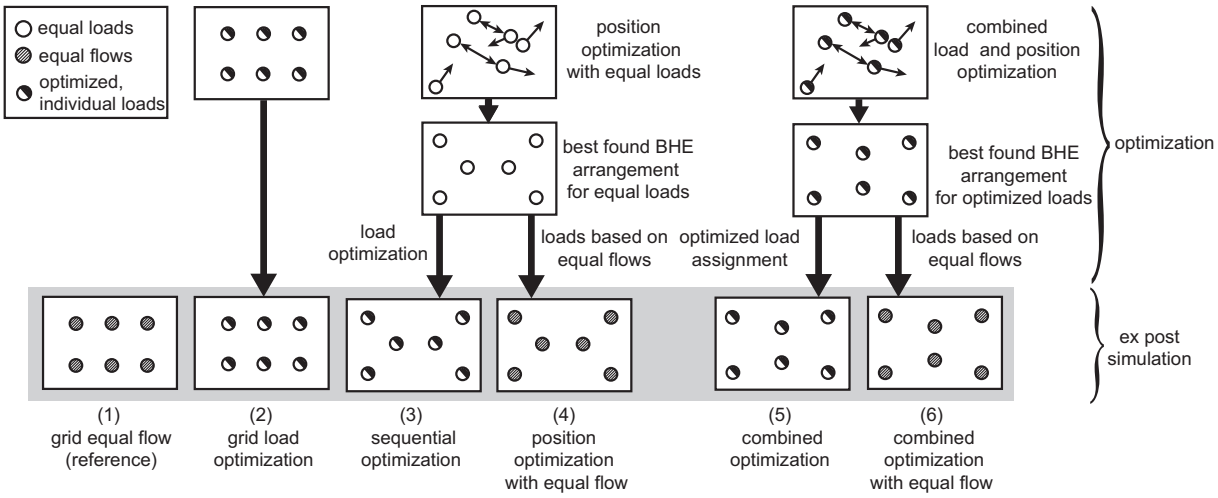

Fig. 6. Six strategies which are employed during the optimization/simulation procedure.

examine the consequences, if borehole fields, which are geometrically optimized with adjusted loads, are operated with equal flows.

The size and the calculation time of the coefficient matrices holding the $\omega_{k,l}^{t,i,j}$ increase quadratically with the number of distinguished time steps m. In addition, the runtime of the linear program solver, which determines the global optimal load assignment for a BHE constellation, rises tremendously with larger coefficient matrices. This means, even when exploiting the symmetries, a single month by month load optimization for a period of 30 years requires a calculation time of several minutes. For computational reasons, when comparing the six strategies, loads are not optimized on monthly resolution, but for the entire operation period of 30 years as one single time step with an averaged heat transfer rate. The averaged load corresponds to the average of the load pattern shown in Fig. 2. This simplification means a speedup by a factor of about 1000, for an optimization run with 50,000 objective function calls. In this way, the runtime for combined load and BHE position optimization can be kept within 20 h on an AMD Opteron system (2.4 GHz, 32 GB of RAM).

3. Results

For the numerical ex-post simulation step, in each case we select the best found solution of the preceding optimization step. The quality of optimized borehole fields is of primary interest to judge the efficiency of the compared strategies. In accordance with the objective function, we chose $\max(\Delta\overrightarrow{T}_{i,j})$, the maximum reached temperature decrease in the underground at the end of the simulation time of 30 years, as quality criterion. Fig. 7 shows the results of the six strategies as depicted in Fig. 6.

The reference case, "grid equal flow", is the non-optimized grid constellation (strategy (1)). During the operation time of 30 years, ground temperature decreases by 10.5 K around the central BHEs in the field. This reveals a significant impact from heat extraction on the thermal regime in the ground, which means conditions close to the freezing point in central European climates. Taking $\max(\Delta\overrightarrow{T}_{i,j})$as criterion, the different optimization strategies all improve the system's performance by mitigation of ground cooling. Still, the differences between optimized solutions and reference are not exorbitant, and an improvement potential of about 1 K (i.e. about 10%) is observed in the results shown in Fig. 7.

The "grid load optimization" (strategy (2)), which only involves load optimization by linear programming, already achieves $\Delta T = 9.5$ K, which is close to the best solution achieved by any other strategy. Fig. 7 illustrates that for the other strategies, which involve heuristic position optimization, the 20 repeated optimization runs deliver a range of solutions with different quality. While load optimization by linear programming always finds the global optimum, repeated applications of the stochastic DE algorithm are needed when BHE positions are adjusted. However, the boxplots in Fig. 7 only span a small range, which reveals a robust performance of the DE. This is particularly the case for position optimization with sequential load adjustment (strategy (3)) and with equal flows (strategy (4)). The results for strategy (3) demonstrate that load optimization on a BHE grid is nearly as good as for a pre-optimized BHE layout. In other words, this shows that geometric arrangement and BHE-specific heat extraction can be similarly utilized for

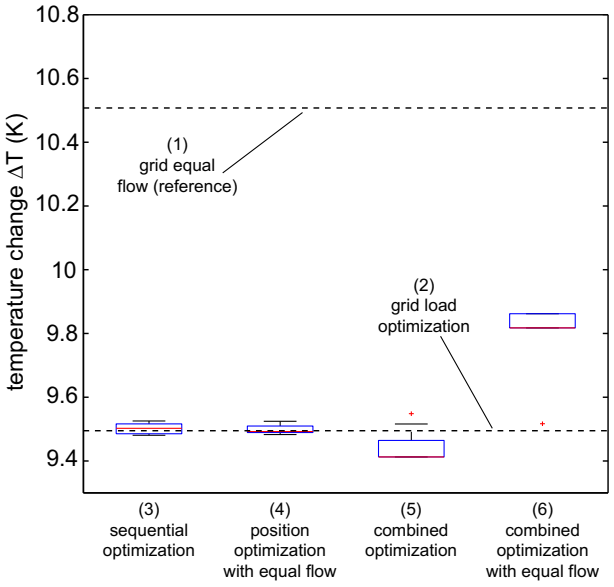

Fig. 7. The boxplots show median and dispersion of the biggest temperature changes in the field of the 20 optimization runs for each strategy. The largest temperature changes are determined after the ex-post simulation with SBM as described in Section 2.3 (Fig. 4). All strategies have in common that the biggest temperature changes occurred close to the BHEs positioned in the center of the field.

accessing the heat available in the subsurface and to obtain balanced thermal ground conditions. Apparently, a badly arranged borehole field can be compensated by proper individual BHE loads. Alternatively, optimized BHE layout works nearly optimal with equal flows. Strategy (4) even shows that little differences exist if equal flows are applied. We can conclude that in practice, load optimization and potentially demanding BHE-specific operation is not required, if the geometric arrangement of the BHEs has been optimized when the field is installed. Load optimization, however, is attractive for given, e.g. grid-shaped, BHE layouts.

For strategies (3) and (4), the BHE position optimization step converged to a small number of characteristic geometric arrangements. In detail, 45% of the optimization runs found scheme a) as depicted in Fig. 8. The remaining 55% converged to the BHE scheme b). Both schemes share similar properties, the concentration of most of the BHEs at the fringe of the feasible positioning square, and only 4 (i.e. 1 per quadrant) regularly oriented BHEs within the square. This demonstrates that it is advantageous to position BHEs away from the very competitive central square, in order to maximize conductive heat flow towards the field from the ambient ground. This is beneficial for the entire system even if the resulting small distance between the outer BHEs may enhance undesirable interaction between neighbors.

Load optimization with the more symmetric scheme a) (Fig. 8) yields a solution with equal loads for all BHEs in the fields. For arrangement b), the sequentially optimized BHE loads vary in a range of 3 W m^{-1} with highest energy extraction by the BHEs in the corners of the field. Again, this highlights the small, further optimization potential, once the positions are adjusted, and is also described by the small differences between all optimization results from strategies (3) and (4) (Fig. 7) with a spread of ΔT in a range of <0.1 K for both.

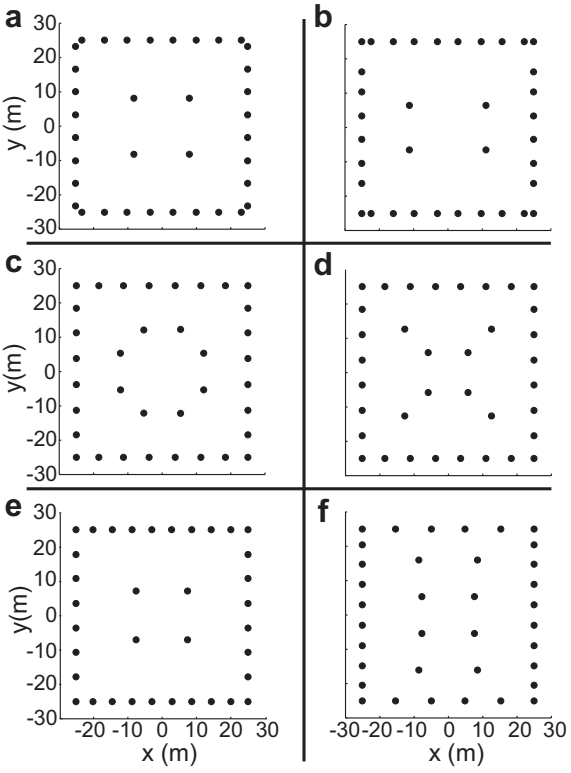

Fig. 8. BHE arrangements of the best optimization runs. Arrangements a) and b) result from the strategies 1 and 2, arrangements c)–f) from the "combined optimization" strategies (Strategy 5 and 6).

Best solutions are expected from a procedure that combines position and load tuning, instead of separating the methods in a sequential procedure. The computationally demanding combined optimization strategy (5) in fact delivers improved solutions with lowest $\Delta T = 9.4$ K. For this strategy we can distinguish four different characteristic schemes (Fig. 8c)–f)) of the BHEs in the field. Fig. 8e) shows one layout similar to those found in the sequential procedure (Fig. 8a) and b)). Again, only 4 BHEs are positioned within the square. However, in scheme 8e), the BHEs along the fringe are all set at equal distance. The other schemes allow 8 of the 36 BHEs regularly arranged as circle (Fig. 8c)), cross (8d)) or rectangle (8f)) within the square. The optimized workloads of the BHEs for arrangements 8c)–8f) show a distribution similar to the optimized workloads for arrangement 8b), with loads varying in a range of 3–4 W m^{-1} and with the highest loads in the corners of the fields. Thus, it seems that the smallest possible temperature changes in the field are only achievable by an unequal operation mode.

A crucial finding is that the computationally demanding combined heuristic-linear optimization procedure is very successful, and outliers with inacceptable sub-optimal solutions were rare. The combined solutions show a slightly greater ΔT spread than those for the sequential procedure (Fig. 7), but generally are better. This is an indication that an exclusive load or position adjustment does not tap the full optimization potential. Strategy (6) inspects what happens if the strategy (5) solutions (schemes c)–f), Fig. 8) are operated with equal flow. The results are substantially worse than the optimal ones with tuned loads. This means that a solution found with the combined optimization procedure has to be operated by the given loads and exhibits a small flexibility.

To further inspect the role of BHE operation mode, we once again simulated the six identified BHE schemes in Fig. 8 numerically with the program SBM at monthly resolution (360 time steps) with both optimized loads and equal flows. This means a total number of 14 demanding simulations, that is seven simulations with equal flows and another seven with optimized loads (arrangements a)–f) plus the grid arrangement, Figs. 1 and 8). Fig. 9 shows the resulting temperature changes in the ground. Fig. 10 offers a top view at the conditions in 50 m depth. The obtained values of $\max(\Delta T_{i,j})$ are about 2 K higher than for the simulations with one single time step for the complete 30 years and an averaged load profile. This results from the effect that a month-wise simulation of the given load profile (Fig. 2) considers annual oscillations of the ground temperature, with a difference of nearly 4 K between coldest temperatures in the winter months and

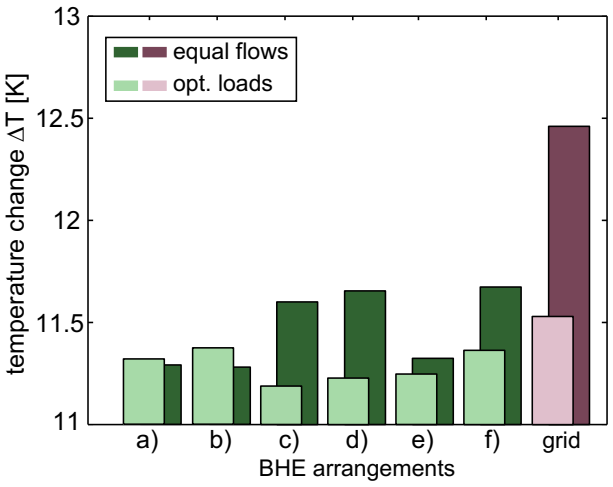

Fig. 9. Resulting minimum temperature changes in the ground if month-wise simulation is applied on the six BHE arrangements depicted in Fig. 8.

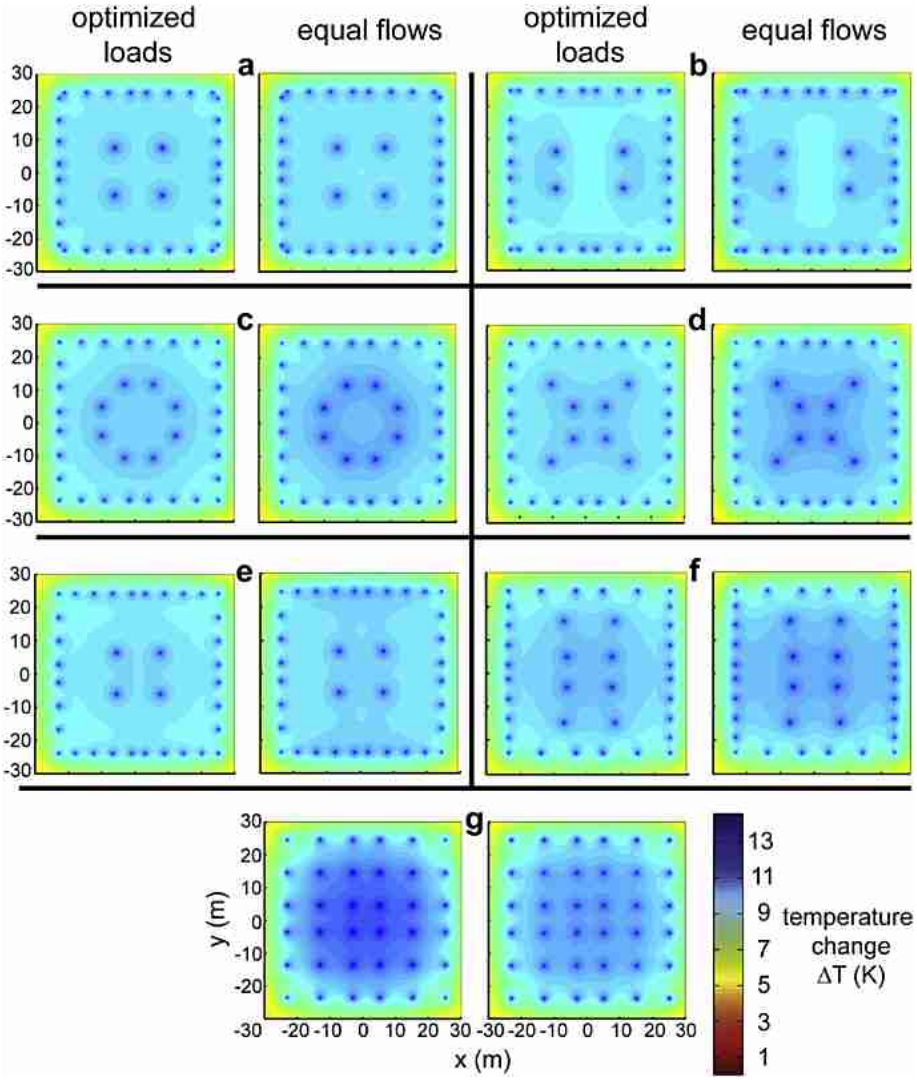

Fig. 10. Distribution of temperature changes in the subsurface (50 m) after 30 years of simulation for the BHE arrangements shown in Fig. 8 for the optimized load and the equal flow case.

highest temperatures in the summer months, while simulations with an averaged load profile only consider the average temperature of the whole year, which lies at the median of the seasonal peaks. Similar trends have been presented by Signorelli et al. [44] for a one-year simulation period with different time resolution, and related work on the effect of load aggregation is available e.g. by Yavuzturk [49,50].

The month-wise simulations confirm the results, which were achieved with the simplified simulations with one single time step and an averaged load profile. The least ground cooling can only be achieved with the four schemes (Figs. 8 and 10 c–f) found by the combined strategy (5), given that these schemes are operated with variable, optimal BHE loads. All four constellations induce higher temperature changes in the ground if the BHEs are operated with equal flows. From these four constellations, BHE arrangement 8e) shows the least temperature change increase when operated with equal flows. This can be explained by the fact that it is shaped very similar to arrangement 8a) and b), which are detected by strategy (3), which operate all BHEs with equal loads during the position optimization step.

Arrangements 8a) and b), which were identified employing sequential strategy (3), show a little higher temperature changes when the BHEs are operated with variable, optimal loads. However, these inconsistencies lie in a range of 0.1 K or less and can be attributed to the discrepancies of the models and the loss of precision due to the interpolation we used to evaluate the temperature outputs of SBM (see Section 2.3). Fig. 10 visualizes the achieved more smoothened temperature distribution in the ground for all geometric optima. Local cooling is mitigated by favoring BHE positions at the fringe. Temperatures of load-optimized and equal flow results apparently are only slightly different, which demonstrates that further optimization potential is small once the geometric arrangement is ideally adjusted (see Fig. 7). Accordingly, strongest temperature changes are observed for the grid arrangement with equal flows (Fig. 10g), the case which is standard in practice.

4. Conclusions

We examined different ways of adjusting BHEs in large borehole fields. In such a field, multiple BHEs are installed to supply a given seasonal energy demand. By joint use of several neighboring BHEs a greater volume of the ground is accessed than by a single BHE system. However, the BHEs may interfere and thus joint operation

is different to application of isolated single systems. Accordingly, the challenge of joint operation is an increase of energy extraction, rather than finding an optimal strategy of concerted BHE use. Our idea is to combine two degrees of freedom, which so far are unexploited in practice. One is to regulate the energy extraction or load per BHE individually, and by this achieve a balanced cooling of the ground. The other is to identify a geometric arrangement of a given number of BHEs to ideally extract the energy of a given volume of the ground. Both steps are formulated as separate and combined optimization problems, and the results for a synthetic 36 BHE field are inspected. For optimization and analysis of results, superimposed analytical finite line-source models and a numerical model are employed. Load optimization is solved by linear programming, whereas the non-linear BHE positioning task is tackled by an Evolutionary Algorithm.

One main result is that the best solutions found improve standard practice. Best solutions require BHE loads that are adjusted to a certain geometric constellation of the BHEs. Still, the gain from optimization for the studied hypothetical example case is moderate. Given the seasonally variable heat demand, maximum temperature in the ground can be mitigated by 10–15%. This benefit has to be contrasted with the additional investment necessary for month-wise BHE load regulation, which is necessary for realizing optimal solutions in practice. However, it is demonstrated that the difference between fields with load-optimized and those with location optimized equal flow BHEs is not significant. Both optimization procedures result in focused energy extraction at the fringe of the field in order to enhance lateral energy replenishment. Load-optimized designs with BHEs oriented on standard grids thus emphasize those BHEs at the boundaries. Location optimization shows a favor of BHE concentrated along the field's border. The shapes of the found optimal arrangements and the number of BHEs positioned in the central regions of the given area depend on different criteria, such as presence of groundwater flow or if additional variable load regulation is possible [32]. If both criteria are fulfilled, it may be favorable to move some BHEs from the fringe to the central areas of the field, because the cooling in the center of the field can be more outbalanced by additional advective energy provision and variable BHE workloads.

One conclusion is that by a priori choosing a strategic BHE arrangement the long-term performance of the system can be improved, without load regulation and associated additional investments. In future work, further improvement of standard practice and the effects on the cooling of the ground should be investigated by integrating heat injection, in the ground during the regeneration season. Also coupling with other systems, like solar collectors in hybrid systems could be optimized by the presented methodology.

Acknowledgments

This work was supported by the German Federal Environmental Foundation (DBU), the Landesstiftung Baden-Württemberg and the Federal Ministry for Education and Research (BMBF) scholarship program for International Postgraduate Studies in Water Technologies (IPSWaT) and the EU FP7 ECO-GHP project. Special thanks go to Gabi Moser for language corrections, and to two reviewers that helped to improve the paper.

References

[1] Ferguson G. Characterizing uncertainty in groundwater-source heating and cooling projects in Manitoba, Canada. Energy 2012;37:201–6.
[2] Kalogirou SA, Florides GA, Pouloupatis PD, Panayides I, Joseph-Stylianou J, Zomeni Z. Artificial neural networks for the generation of geothermal maps of ground temperature at various depths by considering land configuration. Energy 2012;48(1):233–40.
[3] Zheng G, Li F, Tian Z, Zhu N, Li Q, Zhu H. Operation strategy analysis of a geothermal step utilization heating system. Energy 2012;44:458–68.
[4] Ungemach P, Antics M. The road ahead toward sustainable geothermal development in Europe. In: Proceedings World Geothermal Congress 2010, Bali, Indonesia.
[5] Hecht-Méndez J, Molina-Giraldo N, Blum P, Bayer P. Evaluating MT3DMS for heat transport simulation of closed geothermal systems. Ground Water 2010; 48(5):741–56.
[6] Bayer P, Saner D, Bolay S, Rybach L, Blum P. Greenhouse gas emission savings of ground source heat pump systems in Europe: a review. Renewable and Sustainable Energy Reviews 2012;16(2):1256–67.
[7] Karytsas C. Current state of the art of geothermal heat pumps as applied to buildings. Advances in Building Energy Research 2012;6(1).
[8] Mottaghy D, Dijkshoorn L. Implementing an effective finite difference formulation for borehole heat exchangers into a heat and mass transport code. Renewable Energy 2012;45:59–71.
[9] Bloomquist RG. Geothermal heat pumps four plus decades of experience. Geo-Heat Centre Quarterly Bulletin 1999;20(4):13–8.
[10] Preene M, Powrie W. Ground energy systems: from analysis to geotechnical design. Geotechnique 2009;59:261–71.
[11] Omer AM. Ground-source heat pumps systems and applications. Renewable and Sustainable Energy Reviews 2008:344–71.
[12] Fan R, Jiang Y, Yao Y, Ma Z. Theoretical study on the performance of an integrated ground-source heat pump system in a whole year. Energy 2008;8: 1671–9.
[13] Kim S, Bae G, Leen K, Song Y. Field-scale evaluation of the design of borehole heat exchangers for the use of shallow geothermal energy. Energy 2010;35: 491–500.
[14] Zanchini E, Lazzari S, Priarone A. Long-term performance of large borehole heat exchanger fields with unbalanced seasonal loads and groundwater flow. Energy 2012;38:66–77.
[15] Younis M, Bolisetti T, Ting D. Ground source heat pump systems: current status. International Journal of Environmental Studies 2010; 67(3):405–15.
[16] Haehnlein S, Bayer P, Blum P. International legal status of the use of shallow geothermal energy. Renewable and Sustainable Energy Reviews 2010;14(9): 2611–25. http://dx.doi.org/10.1016/j.rser.2010.07.069.
[17] Carslaw HS, Jaeger JC. Conduction of heat in solids. New York, NY, USA: Oxford University Press; 1959.
[18] Brielmann H, Lueders T, Schreglmann K, Ferraro F, Blum P, Bayer P, et al. Oberflächennahe Geothermie und ihre potentiellen Auswirkungen auf die Grundwasserökologie. Grundwasser 2011;16(2):77–91.
[19] Johnston I, Narsilio G, Colls S. Emerging geothermal energy technologies. KSCE Journal of Civil Engineering 2011;14(4):643–53.
[20] Banks D. An introduction to thermogeology: ground source heating and cooling. Oxford: Blackwell Publishing; 2008.
[21] Ochsner K. Geothermal heat pumps: a guide for planning and installing. Earthscan Publications Ltd; 2007.
[22] Sanner B, Mands E, Sauer MK. Larger geothermal heat pump plants in the central region of Germany. Geothermics 2003;32:589–602.
[23] Cross S, Eagan D, Tolme P. Going underground on campus: tapping the earth for clean, efficient heating and cooling. Technical report, National Wildlife Federation, 2011. www.nwf.org.
[24] Witte HJL, van Gelder AJ, Klep P. A very large distributed ground source heat pump project for domestic heating: schoenmakershoek, Etten-Leur (The Netherlands). Proceedings Ecostock, the Tenth International Conference on Thermal Energy Storage. In Richard Stockton College, New Jersey, 2006. http://www.groenholland.com/nl/publications/.
[25] Yu X, Wang R, Zhai XQ. Year round experimental study on a constant temperature and humidity air-conditioning system driven by ground source heat pump. Energy 2011;36:1309–18.
[26] Teza G, Galgaro A, de Carli M. Long-term performance of an irregular shaped borehole heat exchanger system: Analysis of real pattern and regular grid approximation. Geothermics 2012;43:45–56.
[27] Bakirci K. Evaluation of the performance of a ground-source heat-pump system with series GHE (ground heat exchanger) in the cold climate region. Energy 2010;35:3088–96.
[28] de Paly M, Hecht-Mendez J, Beck M, Blum P, Zell A, Bayer P. Optimization of energy extraction for closed shallow geothermal systems using linear programming. Geothermics 2012;43:57–65.
[29] Hecht-Méndez J, de Paly M, Beck M, Bayer P. Optimization of energy extraction for vertical closed-loop geothermal systems considering groundwater flow. Energy Conversion and Management 2013;66:1–10.
[30] Beck M, Hecht-Mendez J, de Paly M, Bayer P, Blum P, Zell A. Optimization of the energy extraction of a shallow geothermal system. In: Proceedings of the IEEE Congress on Evolutionary Computation (CEC), Barcelona, Spain, 2010: 3622–8.
[31] Bürger C, Bayer P, Finkel M. Algorithmic funnel-and-gate system design optimization. Water Resources Research 2007;43.
[32] Beck M, de Paly M, Hecht-Mendez J, Bayer P, Zell A. Evaluation of the performance of evolutionary algorithms for optimization of low-enthalpy geothermal heating plants. In: Proceedings of the ACM Genetic and evolutionary computation Conference (GECCO), Philadelphia, USA, 2012.

[33] Eskilson P. Thermal analysis of heat extraction boreholes. Doctoral thesis, 1987.
[34] Pahud DAF, Hadorn JC. The superposition borehole model for TRNSYS (TRNSBM). User Manual for the November 1996 version. Internal Report in LASEN-DGC-EPFL, Switzerland, 1996.
[35] Nordell B, Hellström G. High temperature solar heated seasonal storage system for low temperature heating of buildings. Solar Energy 2000;69:511–23.
[36] Molina-Giraldo N, Blum P, Zhu K, Bayer P, Fang Z. A moving finite line source model to simulate borehole heat exchangers with groundwater advection. International Journal of Thermal Sciences 2011;50(12):2506–13. http://dx.doi.org/10.1016/j.ijthermalsci.2011.06.012.
[37] Hellström G. Ground heat storage: thermal analysis of duct storage systems. Lund: Department of Mathematical Physics, University of Lund; 1991.
[38] Yavuzturk C, Spitler JD, Rees SJ. A transient two-dimensional finite volume model for the simulation of vertical U-tube ground heat exchangers. ASHRAE Transaction 1999;105(2):465–74.
[39] Diao N, Li Q, Fang Z. Heat transfer in ground heat exchangers with groundwater advection. International Journal of Thermal Sciences 2004;43(12): 1203–11.
[40] Michopoulos A, Kyriakis N. A new energy analysis tool for ground source heat pump systems. Energy and Buildings 2009;41(9):937–41. http://dx.doi.org/10.1016/j.enbuild.2009.03.017.
[41] Marcotte D, Pasquier P, Sheriff F, Bernier M. The importance of axial effects for borehole design of geothermal heat-pump systems. Renewable Energy 2010; 35(4):763–70. http://dx.doi.org/10.1016/j.renene.2009.09.015.
[42] Bernier MA, Pinel P, Labib R, Paillot R. A multiple load aggregation algorithm for annual hourly simulations of GCHP systems. HVAC & R Research 2004; 10(4):471–88.
[43] Marcotte D, Pasquier P. Fast fluid and ground temperature computation for geothermal ground-loop heat exchanger systems. Geothermics 2008;37(6): 651–65. http://dx.doi.org/10.1016/j.geothermics.2008.08.003.
[44] Signorelli S, Kohl T, Rybach L. Sustainability of production from borehole heat exchanger fields. In: Proceedings, Twenty-Ninth Workshop on Geothermal Reservoir Engineering, Stanford University, Stanford, California, 2004.
[45] Ingenieure VD, editor. VDI, Thermische Nutzung des Untergrundes, teil 2. Düsseldorf: VDI-Verlag; 2001.
[46] Florides GA, Christodoulides P, Pouloupatis P. An analysis of heat flow through a borehole heat exchanger validated model. Applied Energy 2012;92:523–33.
[47] Bayer P, Bürger C, Finkel M. Computationally efficient stochastic optimization using multiple realizations. Advances in Water Resources 2008; 31(2):399–417.
[48] Bayer P, de Paly M, Bürger C. Optimization of high-reliability based hydrological design problems by robust automatic sampling of critical model realizations. Water Resources Research 2010;46.
[49] Yavuzturk C, Spitler JD. A short time step response factor model for vertical ground loop heat exchangers. ASHRAE Transactions 1999;105(2):475–85.
[50] Fisher DE, Rees SJ, Padhmanabhan SK, Murugappan A. Implementation and validation of ground-source heat pump system models in an integrated building and system simulation environment. HVAC & R Research 2006; 12(S1):693–710.